

Adiabatic approximations to internal rotation

Wesley D. Allen^{a)}*Center for Computational Chemistry, University of Georgia, Athens, Georgia, 30602*

Andras Bodi

Laboratory of Molecular Spectroscopy, Institute of Chemistry, Eötvös University, P.O. Box 32, H-1518 Budapest 112, Hungary

Viktor Szalay

*Crystal Physics Laboratory, Research Institute for Solid State Physics and Optics, Hungarian Academy of Sciences, P.O. Box 49, H-1525 Budapest, Hungary*Attila G. Császár^{b)}*Laboratory of Molecular Spectroscopy, Institute of Chemistry, Eötvös University, P.O. Box 32, H-1518 Budapest 112, Hungary*

(Received 6 March 2006; accepted 1 May 2006; published online 12 June 2006)

A number of subtle and confusing issues are addressed concerning large amplitude motion (LAM) coordinates (χ) for internal molecular motions, using the methyl rotation in acetaldehyde (CH_3CHO) as a model problem. If the LAM coordinate is chosen to be one of the H–C–O dihedral angles ρ_1 , ρ_2 , or ρ_3 , it lacks the required $2\pi/3$ periodicity, and its use is thus undesirable. An excellent local internal coordinate for this model problem is $\tau_3 = \frac{1}{3}(\rho_1 + \rho_2 + \rho_3 - 2\pi)$. A similarly good but nonlocal coordinate for the adiabatic approximation of internal rotation is provided by the intrinsic reaction coordinate s . Comparison of the mass-independent $V_0(\tau_3)$ and the mass-dependent $V_0(s)$ internal rotation curves shows that the two are virtually identical for the parent isotopolog of acetaldehyde. A unified internal coordinate projection scheme for determining complementary vibrational frequencies and subsequently $V_{\text{ZPVE}}(\chi)$ along a path for LAM has been formulated, where $V_{\text{ZPVE}}(\chi)$ is the zero-point vibrational energy correction to the internal rotation curve. In addition to its simplicity, the projection scheme developed for a distinguished reaction path generated by constrained optimizations is appealing because the vibrational frequencies along the LAM path are invariant to chemically meaningful choices of the internal coordinates for the complementary modes. © 2006 American Institute of Physics. [DOI: [10.1063/1.2207614](https://doi.org/10.1063/1.2207614)]

I. INTRODUCTION

The earliest experimental and theoretical attempts to elucidate the molecular phenomenon of internal rotation date back to the 1930s.^{1,2} Internal rotation is a large amplitude motion^{3–12} (LAM) along a curvilinear path and is not amenable to the classic perturbative treatment of normal mode vibrations about a single potential energy minimum. Often a separation of time scales allows a sudden/adiabatic approximation wherein the dimensionality of the Hamiltonian is reduced by vibrational averaging of the fast, small-amplitude motions for each value of the coordinate for slow internal rotation.

It makes no difference how the coordinates describing internal rotations are defined as long as one employs an exact rotational-vibrational Hamiltonian and solves the corresponding Schrödinger equation exactly. However, in practice for all cases but the dynamics of few-body systems, one has to introduce approximations. The general technique^{6,13–15} often employed by spectroscopists is as follows. In the relevant region of the potential energy surface, approximations to the exact Hamiltonian are made by truncated Taylor series ex-

pansions with respect to the small-amplitude vibrational coordinates, without any expansion with respect to the LAM coordinate. Since the Schrödinger equation built upon this approximate Hamiltonian is amenable to neither an exact analytical nor an efficient numerical solution, further simplifications are needed. To proceed, one orders, through the so-called Born-Oppenheimer parameter,¹⁶ the various terms in the Hamiltonian according to the estimated magnitude of their contribution to the molecular energy. Next, under the assumption that the rotational and LAM characteristic frequencies are much lower than those of the small-amplitude vibrations, the approximate Hamiltonian is transformed by unitary transformations. This transformation corresponds to folding some of the off-diagonal matrix elements, which would be obtained when calculating the Hamiltonian matrix elements by using the eigenfunctions of the zeroth-order small-amplitude vibrational Hamiltonian as basis functions, into the main diagonal. The transformed Hamiltonian is again ordered and truncated to keep only terms up to second order. Averaging this Hamiltonian with respect to the zeroth-order, small-amplitude vibrational eigenstates gives an effective rotational LAM Hamiltonian accounting for coupled, complementary vibrations to second order in the Born-

^{a)}Electronic mail: wallen@ccqc.uga.edu^{b)}Electronic mail: csaszar@chem.elte.hu

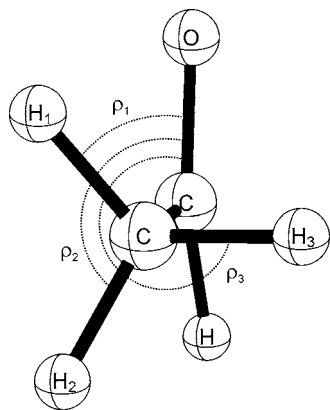


FIG. 1. Dihedral angles ρ_1 , ρ_2 , and ρ_3 in acetaldehyde.

Oppenheimer parameter.³ The Schrödinger equation built upon this effective Hamiltonian can be solved numerically.

In what follows we shall concentrate on the adiabatic approximation concerning a single LAM coordinate, χ . For a nonlinear N -atomic molecule the zeroth-order effective, adiabatic LAM potential, $V(\chi)$, can be expressed as

$$V(\chi) = V_0(\chi) + V_{\text{ZPVE}}(\chi) = V_0[\mathbf{a}(\chi)] + \frac{1}{2} \sum_{k=1}^{3N-7} \omega_k(\chi). \quad (1)$$

In this equation $\mathbf{a}(\chi)$ is the Cartesian molecular geometry along the LAM path, and the small-amplitude vibrations are assumed to be harmonic with corresponding frequencies $\omega_k(\chi)$. For simplicity we have also assumed in Eq. (1) that all small-amplitude vibrations are in their respective ground state. Subscript ZPVE stands for the zero-point vibrational energy of the complementary modes, and $V_0(\chi)$ is the LAM reference potential devoid of modulation from orthogonal vibrations.

As evident from the related literature on large amplitude motions^{14,17,18} and reaction path dynamics,¹⁹⁻²¹ there is no unique prescription for selecting the LAM coordinate χ . Nevertheless, it is crucial to define χ properly and in accord with the approximations invoked to arrive at Eq. (1). In the case of internal rotation, there are a number of subtle and confusing issues regarding the choice of χ , and simple intuition can be misleading. Spectroscopists have preferred the use of locally defined internal coordinates for the description of internal rotation. It has been found^{17,18} that in the case of acetaldehyde, CH_3CHO , the internal rotation potential, $V_0(\chi)$, of the methyl group determined by electronic structure computations assuming the χ to be one of the H-C-C-O dihedral angles ρ_1 , ρ_2 , or ρ_3 (see Fig. 1) lacks the intuitive $2\pi/3$ periodicity that has been substantiated by analyses of experimental spectroscopic data. On the other hand, high-level, converged *ab initio* computations employing the most suitable internal coordinate for the methyl torsion of acetaldehyde,

$$\tau_3 = \frac{1}{3}(\rho_1 + \rho_2 + \rho_3 - 2\pi), \quad (2)$$

gave torsional frequencies and a contortional parameter^{17,22} that were in excellent agreement with the corresponding experimental data.²³

One way of avoiding inappropriate χ definitions for internal rotation is to use the arc length (s) of the intrinsic reaction path (IRP) traced in the $3N$ -dimensional configuration space of mass-weighted Cartesian coordinates (\mathbf{q}) of the atoms. This arc length is the intrinsic reaction coordinate (IRC),²⁴⁻²⁶ a nonlocal coordinate, and the associated path in \mathbf{q} space is defined by the differential equation

$$\frac{d\mathbf{q}}{ds} = -\frac{\mathbf{g}_q}{|\mathbf{g}_q|}, \quad (3)$$

where $\mathbf{g}_q = \partial V / \partial \mathbf{q}$ is the potential energy gradient along the IRP. In this paper, we generalize this differential equation to describe other χ coordinates and associated paths, including those typically generated by constrained optimizations of a so-called distinguished reaction coordinate (DRP).²⁷

The computation of $V_{\text{ZPVE}}(\chi)$ from *ab initio* force fields has often been a vexing problem in theoretical chemistry. Previous groundbreaking work has developed elegant and practical formalisms to attack this problem both in Cartesian and internal coordinate spaces.^{10-12,28-31} Here we present a unified internal coordinate projection scheme for the evaluation of vibrational frequencies along LAM paths and highlight an appealing approach to this problem for distinguished reaction coordinates. Recent discussions^{32,33} on $V(\chi)$ of acetaldehyde serve to emphasize the importance of these topics.

II. COMPUTATIONAL DETAILS

The principles under discussion in this paper can be exemplified at any level of electronic structure theory. For the sake of simplicity, the availability of analytic first and second derivatives, and added numerical precision for analysis of fine details, the computations presented here were performed using restricted Hartree-Fock³⁴ (RHF) and second-order Møller-Plesset³⁵ (MP2) theory with the standard 6-31G(d,p) basis set.³⁶

The program suites GAUSSIAN 98³⁷ and GAUSSIAN 03³⁸ were used to produce the synchronous transit-guided quasi-Newton³⁹ (STQN) path. Intrinsic reaction coordinate^{19,24-26} (IRC) computations were performed with the PC GAMESS version⁴⁰ of the GAMESS (US) quantum chemistry package.⁴¹ The program system ACES II⁴² was used to execute constrained geometry optimizations to map $V_0(\chi)$ along DRPs.²⁷ The analytic fits to the *ab initio* $V_0(\chi)$ data were performed using the computer algebra system MATHEMATICA.⁴³

Vibrational frequencies and ZPVEs along the internal rotation paths were calculated using several formalisms. All the formalisms for vibrational analysis in the orthogonal-complement space along a general path are supported by INTDER2005.⁴⁴⁻⁴⁶ The built-in feature Freq(Projected) of GAUSSIAN 03 was also used for standard projected frequency analyses in mass-weighted Cartesian coordinates along the intrinsic reaction path.

To ensure reproducibility of our results, we report the internal coordinates \mathbf{S} used in all of our projected vibrational frequency analyses of acetaldehyde: all six bonded distances, five nonredundant symmetry adapted linear combinations of

TABLE I. Fourier coefficients of various $V_{0,\chi}$ internal rotation curves of acetaldehyde, fitted to the common representation of Eq. (6) with $\theta=\tau_3$, unless otherwise specified.

Level of theory	LAM coordinate ^a	V_3/cm^{-1}	V_6/cm^{-1}	V_9/cm^{-1}	rms error/ cm^{-1}
RHF/6-31G(<i>d,p</i>)	IRC	373.197	-9.705	+0.001	$4.2 \cdot 10^{-3}$
	τ_3	373.120	-10.173	+0.079	$6.26 \cdot 10^{-3}$
	STQN	373.379	-8.096	-0.178	$4.93 \cdot 10^{-3}$
	IRC' (unit masses)	373.362	-8.037	-0.181	$5.46 \cdot 10^{-3}$
	ρ_1	373.356	-8.035	-0.151	$1.39 \cdot 10^{-1}$
	ρ_1 ($\theta=\rho_1$)	372.323	-12.102	+0.613	8.00
MP2/6-31G(<i>d,p</i>)	IRC	363.537	-11.221	+0.046	$7.6 \cdot 10^{-3}$
	τ_3	363.428	-11.724	+0.152	$6.52 \cdot 10^{-3}$
	STQN	363.797	-9.391	-0.219	$2.06 \cdot 10^{-2}$
	IRC' (unit masses)	363.756	-9.412	-0.174	$9.71 \cdot 10^{-3}$

^aSee text for the definition of the coordinates.

the six (H–C–H and H–C–C) bond angles of the methyl group, two combinations of the three (C–C–O, C–C–H, and H–C–O) bond angles in the formyl group, the H–CCO out-of-plane angle, and the τ_3 coordinate of Eq. (2). Specifically, we used the natural internal coordinates recommended by Fogarasi *et al.*⁴⁷

III. INTERNAL ROTATION POTENTIAL ENERGY CURVES

In this paper the methyl internal rotation of acetaldehyde is used as an example to demonstrate the advantages and disadvantages of some of the most widely employed internal rotation coordinates χ for generation of $V_0(\chi)$. While the construction and the shape of $V_0(\chi)$ varies with the chosen LAM coordinate, $V_0(\chi)$ is fundamentally acquired by scanning the curve over selected values of χ . Each choice of LAM coordinate effectively constitutes a different adiabatic approximation for the separation of large- and small-amplitude motions. The effect of various χ choices on the LAM potential energy curves is documented in Table I.

A. Simple dihedral angle

The internal rotation coordinate can be chosen to be a simple dihedral angle, defined in the case of acetaldehyde as any one of the H–C–C–O torsion angles (ρ_1 , ρ_2 , or ρ_3 in Fig. 1). Here ρ_i would be fixed and all other coordinates would be optimized to generate a DRP. An obvious advantage of choosing ρ_i to describe the internal rotation is that it is defined locally, allowing the path to be followed with arbitrarily large step sizes. However, choosing a particular ρ_i as a distinguished coordinate for constrained optimizations artificially singles out one of the methyl hydrogens, and thus the resulting $V_0(\rho_i)$ lacks threefold hydrogen equivalence,^{17,18} at variance with the permutation-inversion symmetry of the exact vibrational wave function. For acetaldehyde, the C_3 symmetry of V_0 can be artificially recovered, as done in most previous *ab initio* studies,^{18,48–50} but by methods which either lack theoretical rigor or are rather tedious. For example, $2\pi/3$ periodicity in $V_0(\rho_i)$ might be imposed *post facto* by

fitting this function to an appropriate Fourier series. As argued before¹⁷ and also evident from the results presented in Table I, there are better choices for the internal rotation coordinate.

B. Symmetric combination of dihedral angles

Assuming the validity of the $C_{3v}(\text{M})$ molecular symmetry (MS) group²² for describing the internal rotation in acetaldehyde, and accepting the mathematical consequences of the inability of methyl hydrogens to overtake one another during the rotation,¹⁷ the proper dihedral-angle internal rotation coordinate is τ_3 , as given in Eq. (2). The coordinate τ_3 is still defined locally, and it inherently maintains the expected symmetry, as shown before.¹⁷ No distinction occurs between the dihedral angles describing the methyl hydrogens, and thus the intuitive equivalence of the three hydrogens remains unbroken. Use of τ_3 as the LAM coordinate for acetaldehyde results in a mass-independent potential $V_0(\tau_3)$ of $2\pi/3$ periodicity.

C. Intrinsic reaction coordinate (IRC)

The IRP is defined as the path of steepest descent, in mass-weighted Cartesian coordinates, that emanates from the relevant transition state forward to products and backwards to reactants. The IRC is the signed arc length (s) to a given point along the IRP, with $s=0$ at the transition state, $s>0$ for the product region, and $s<0$ for the reactant region.

One drawback of the IRC for the description of internal rotation is that its evaluation at an arbitrary point cannot be made from local information alone but requires integration of the IRP all the way from the transition state. Another demerit of this choice is the arbitrary assignment of an internal rotation *angle* to the IRC.⁵¹ For example, in acetaldehyde one could set the “rotation angle” to $(2\pi/3)(s/s_{\text{total}})$, where s is the IRC for the given point, and s_{total} is the total arc length from one conformer to the next equivalent one. Alternatively, one could assign the value taken by the τ_3 coordinate [Eq. (2)] at the given point on the IRP. A further disadvantage is that $V_0(s)$ expressed in an IRC becomes mass dependent and thus in principle needs to be recomputed for each isotopolog considered. Finally, because the terminal ap-

proach of the IRP into a potential energy minimum is generally directed along the normal mode of lowest frequency,⁵² unwanted changes in the character of the IRC can result near the endpoints of the internal rotation path, although this phenomenon often occurs too late to be of consequence.

Intrinsic reaction path $V_0(s)$ curves nevertheless have the advantage that the reduced mass is unity when the potential is employed in a one-dimensional solution of the LAM Schrödinger equation. Furthermore, it is the IRC for which the projection procedure for the complementary vibrational modes (*vide infra*) exactly reproduces the usual⁵³ normal-mode description at the stationary points. Weighing the advantages and disadvantages, the IRC provides an excellent coordinate for the adiabatic approximation of the internal rotation.

D. The STQN path method

The STQN path generated by GAUSSIAN 03 was employed by Xu *et al.*³² for their $V_0(\chi)$ for acetaldehyde. The algorithm for obtaining the STQN path has been described in detail in Ref. 39. The STQN procedure uses linear interpolation to construct an initial guess for the path between specified reactants and products. The reaction path is then iteratively refined until the transition state (TS) is located and the paths of steepest descent connecting the TS to the reactant and product are converged upon. The final STQN path fundamentally depends on the coordinate system used in the refinement, the standard choice being a composite set of redundant internal coordinates generated by automation. While the coordinate dependence of the STQN path may be weak in many cases, it is essential to recognize this property and deal with it accordingly.

Two features of the STQN path warrant attention with regard to the internal rotation curve of acetaldehyde: (a) although the usual STQN path is a type of steepest descent trajectory, it is not built upon the mass-weighted Cartesian coordinates, which means that the converged path will deviate from the conventional IRP; and (b) construction of a proper projection operator for obtaining the ZPVE correction corresponding to the small-amplitude complementary vibrations must consider the particular choice of coordinates employed in the STQN algorithm. In previous work,³² there has been some confusion that the path generated with the GAUSSIAN 98 program using the keyword Opt(QST3,Path=43,VTight) is the conventional intrinsic reaction path and that corresponding orthogonal vibrational frequencies should be computed by IRP projection schemes. As discussed below, such a misunderstanding can lead to discontinuities in $V_{\text{ZPVE}}(\chi)$.

E. DRP invariance to complementary coordinates

When choosing a distinguished reaction coordinate for χ , e.g., τ_3 , the question of the 3 $N-7$ complementary coordinates immediately arises. The general transformation equation^{45,46} for gradients in two internal coordinate sets, $\{S_j\}=\{T_i, \chi\}$ and $\{R_k\}=\{U_k, \chi\}$, both containing $3N-6$ coordinates, is

$$\left(\frac{\partial V}{\partial R_k}\right) = \sum_{i=1}^{3N-6} \left(\frac{\partial S_i}{\partial R_k}\right) \left(\frac{\partial V}{\partial S_i}\right). \quad (4)$$

Suppose that $\{S_j\}$ is used to generate the internal rotation path. Since only the χ variable of $\{S_j\}$ has a nonzero force at the end of the constrained optimization, i.e., $\partial V/\partial T_i=0$, it follows that

$$\left(\frac{\partial V}{\partial U_k}\right) = \left(\frac{\partial \chi}{\partial U_k}\right) \left(\frac{\partial V}{\partial \chi}\right). \quad (5)$$

When taking the partial derivative $\partial \chi/\partial U_k$, by assumption the fixed R_k include χ , so that $\partial \chi/\partial U_k$ must vanish, and thus all the forces $\partial V/\partial U_k$ are zero. In summary, the DRP path generated using complementary coordinates $\{T_j\}$ will not be altered if these coordinates are changed to $\{U_k\}$.

F. Comparison of $V_0(\chi)$ curves

A Fourier representation of our $V_0(\chi)$ curves was constructed by least-squares fitting to the simple three-parameter form

$$V_0[\theta(\chi)] \equiv V_{0,\chi}(\theta) = \frac{1}{2} [V_{3,\chi}(1 - \cos 3\theta) + V_{6,\chi}(1 - \cos 6\theta) + V_{9,\chi}(1 - \cos 9\theta)]. \quad (6)$$

In order to compare various $V_0(\chi)$ curves, a common representation coordinate (θ) for internal rotation must be defined. In most cases we chose $\theta=\tau_3$, since it has the proper symmetry properties, provides a convenient physical description of the internal rotational motion, and is readily evaluated for all choices of χ . The Fourier coefficients for various $V_0(\chi)$ curves are listed in Table I with the root mean square (rms) error of the fit.

In order to quantify the difference between two paths for LAM coordinates χ_1 and χ_2 , a scaled difference integral

$$DI(\chi_1, \chi_2) = \frac{\int_0^{2\pi/3} [V_{0,\chi_1}(\theta) - V_{0,\chi_2}(\theta)]^2 d\theta}{\int_0^{2\pi/3} V_{0,\chi_1}(\theta) d\theta \int_0^{2\pi/3} V_{0,\chi_2}(\theta) d\theta} \quad (7)$$

was employed. Some elements of the matrix of DI values are presented in Table II.

The deviation of the ρ_1 DRP path from the proper C_3 symmetry is evident from the relatively large rms fitting error (Table I) of $V_0(\rho_1)$ to Eq. (6) when $\theta=\rho_1$. This fitting error is a measure of deviation from threefold rotational symmetry because Eq. (6) does not include functions of periodicity less than $2\pi/3$. The problem with $V_0(\rho_1)$ is only partially remedied when the same energy data are fitted using coordinate $\theta=\tau_3$ computed at geometries along the ρ_1 path. All other LAM coordinate choices in Table I yield paths with $2\pi/3$ periodicity, and the corresponding $V_{0,\chi}(\tau_3)$ fits have very small rms errors.

The difference integrals in Table II show that the closest match with the IRC potential curve for the parent isotopolog is obtained with the τ_3 distinguished reaction coordinate. Figure 2 plots the difference between the $V_{0,\chi}(\tau_3)$ curves for the IRC and STQN paths relative to the DRP τ_3 reference curve. Remarkably, the $\Delta E(\tau_3)$ values in the τ_3 -IRP case never exceed 0.5 cm^{-1} . This comparison provides an impor-

TABLE II. Selected difference integrals $DI(\chi_1, \chi_2)$, for internal rotation curves of acetaldehyde.

Level of theory	χ_1	χ_2	$DI \times 10^6$
RHF/6-31G(<i>d,p</i>)	τ_3	IRC	1.21
	τ_3	IRC' (unit masses)	24.61
	τ_3	ρ_1	24.95
	τ_3	STQN	23.58
	ρ_1	STQN	0.02
	IRC	IRC' (unit masses)	14.91
	STQN	IRC	14.11
	STQN	IRC' (unit masses)	0.01
MP2/6-31G(<i>d,p</i>)	τ_3	IRC	1.52
	τ_3	IRC' (unit masses)	31.20
	τ_3	STQN	31.76
	IRC	IRC' (unit masses)	18.98
	STQN	IRC	19.41
	STQN	IRC' (unit masses)	0.01

tant argument in favor of τ_3 as an internal rotation coordinate, especially because it does not have the mass dependency and nonlocal characteristics of the IRC. The $DI(\chi_1, \chi_2)$ data also reveal a noticeable difference between the IRC and IRC' (unit masses) curves, as well as an extremely close match of the STQN potential with its IRC' counterpart.

IV. VIBRATIONAL ENERGY CORRECTION

The zero-point vibrational energy correction $V_{ZPVE}(\chi)$ to the potential function for large-amplitude motion [Eq. (1)] demands careful consideration. $V_{ZPVE}(\chi)$ can account for a significant portion of the adiabatic internal rotation barrier, as observed for the methyl rotation in toluene.⁵⁴ Nevertheless, if the separation of time scales is sufficiently large, even a large ZPVE modulation does not invalidate the adiabatic approximation. Previous computations on acetaldehyde have given a ZPVE contribution to the internal rotation barrier of 2%–5%.^{23,55,56} The computation of $V_{ZPVE}(\chi)$ is often a source of confusion, which has motivated us to formulate a unified internal projection scheme for determining vibrational frequencies along a path for LAM.

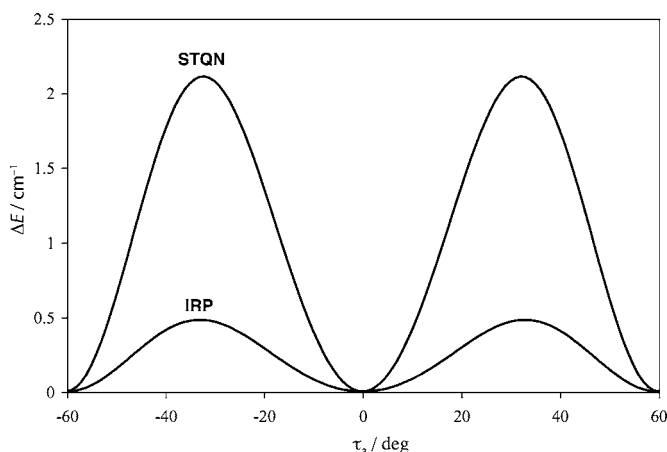


FIG. 2. Energy differences, $\Delta E/\text{cm}^{-1}$, of the intrinsic reaction path (IRP) and the STQN path relative to the τ_3 DRP path for internal rotation in acetaldehyde [RHF/6-31G(*d,p*) level of theory].

A. Internal projection schemes for vibrational analyses

All LAM paths of interest here, even the DRP generated by constrained optimizations, can be considered paths of steepest descent in some (perhaps complicated) coordinate system. The differential equation defining the path of steepest descent for coordinate set \mathbf{R} is

$$\frac{d\mathbf{R}(s)}{ds} = -\frac{\mathbf{g}_R}{\sqrt{\mathbf{g}_R^T \Gamma_{RS} \mathbf{g}_R}}, \quad (8)$$

where \mathbf{g}_R is the corresponding gradient vector, and s is the associated arc length along the path. We may choose to trace the steepest descent path $\mathbf{R}(s)$ in the basis of another coordinate system \mathbf{S} , assumed here to be of dimension f equivalent to the number of internal degrees of freedom of the molecule. In this case Eq. (8) transforms to

$$\frac{d\mathbf{S}_R(s)}{ds} = -\frac{\Gamma_{RS} \mathbf{g}_S}{\sqrt{\mathbf{g}_S^T \Gamma_{RS} \mathbf{g}_S}}, \quad (9)$$

where \mathbf{g}_S is the gradient vector in the new basis, and the subscript on $\mathbf{S}_R(s)$ emphasizes that the path is defined by \mathbf{R} . The matrix Γ_{RS} is given by

$$\Gamma_{RS} = \mathbf{J} \mathbf{J}^T, \quad (10)$$

in which \mathbf{J} is the Jacobian matrix of the transformation from the path-defining \mathbf{R} coordinates to the representation basis \mathbf{S} , i.e., $J_{ij} = (\partial S_i / \partial R_j)$.

For vibrational analyses along the steepest descent \mathbf{R} path, we seek an f -dimensional set $\{Q_1, Q_2, \dots, Q_{f-1}, s\}$ of coordinates whose last component is the arc length s and whose first $f-1$ elements describe complementary normal vibrations about the path. The instantaneous normal displacement coordinates are of the form

$$\mathbf{Q} = \mathbf{M}(s)[\mathbf{S} - \mathbf{S}_R(s)], \quad (11)$$

where $\mathbf{M}(s)$ is an $(f-1) \times f$ transformation matrix. The conditions determining $\mathbf{M}(s)$ are that the gradient vector in the \mathbf{Q} space vanishes at all points along the path, and the quadratic terms for the vibrational kinetic and potential energy are uncoupled in the \mathbf{Q} space. If \mathbf{S} is a nonredundant internal coordinate set, then the formal manipulations that solve for the \mathbf{Q} variables yield a projected variant of the standard El'yashevich-Wilson GF matrix procedure.⁵³ The final prescription for the vibrational analysis is then as follows:

- (1) At each point on the path defined by Eq. (8), compute the kinetic energy matrix \mathbf{G} and the quadratic force constant matrix \mathbf{F} in the \mathbf{S} representation using standard formalisms.
- (2) Form the projection matrix

$$\mathbf{P} = \frac{\mathbf{g}_S \mathbf{g}_S^T}{\mathbf{g}_S^T \Gamma_{RS} \mathbf{g}_S}. \quad (12)$$

- (3) Construct the projected force constant matrix

$$\mathbf{F}_p = (\mathbf{I} - \mathbf{P} \Gamma_{RS}) \mathbf{F} (\mathbf{I} - \Gamma_{RS} \mathbf{P}). \quad (13)$$

- (4) Diagonalize the matrix \mathbf{GF}_p to obtain $f-1$ nonzero frequencies for complementary normal vibrations and one hard zero corresponding to the instantaneous tangent vector on the steepest descent path.

It is important to understand the dual coordinate dependence of the ZPVE-modulated potential function for large-amplitude motion. First, the steepest descent path itself is not invariant to the choice of defining coordinates \mathbf{R} . When the actual computations are performed with an alternative coordinate set, the path definition is merely implicit, and the \mathbf{R} dependence may not be transparent. Second, the vibrational frequencies along the path, and hence the ZPVE contribution to the LAM potential function, depend on the coordinate system \mathbf{S} in which the normal mode analysis is performed. This subtle \mathbf{S} dependence arises because Eq. (8) does not define the value of the LAM coordinate s off the steepest descent path, and the selection of \mathbf{S} indirectly prescribes a particular choice for the lines of constant s in the vicinity of the path. This issue has been discussed previously in the literature^{11,12} in the case of intrinsic reaction paths, where anomalous imaginary vibrational frequencies for complementary normal vibrations sometimes appear if appropriate curvilinear \mathbf{S} coordinates are not employed.

B. Formulas for Γ_{RS}

To implement our unified approach for projected vibrational frequencies along generalized steepest descent paths, formulas must be derived for the Γ_{RS} matrix of Eqs. (9) and (10) for all cases of interest.

Case 1. For a conventional IRP, the path-defining coordinates \mathbf{R} are mass-weighted Cartesians. Thus, $\mathbf{J}=\mathbf{B}_S\mathbf{m}^{-1/2}$, involving the usual \mathbf{B} matrix (\mathbf{B}_S) and the diagonal mass matrix \mathbf{m} . Accordingly, $\Gamma_{RS}=\mathbf{B}_S\mathbf{m}^{-1}\mathbf{B}_S^T=\mathbf{G}_S$, where $\mathbf{G}_S=\mathbf{B}_S\mathbf{m}^{-1}\mathbf{B}_S^T$ is the conventional \mathbf{G} matrix in the internal coordinate set \mathbf{S} . The projection scheme for this case has previously been worked out by Truhlar and co-workers.^{11,12}

Case 2. If the path coordinates \mathbf{R} are an internal coordinate set distinct from the basis \mathbf{S} , then one can apply the chain rule in an intermediate set of Cartesian coordinates to find $\mathbf{J}=\mathbf{G}_{SR}\mathbf{G}_R^{-1}$, where $\mathbf{G}_{SR}=\mathbf{B}_S\mathbf{m}^{-1}\mathbf{B}_R^T$ and $\mathbf{G}_R=\mathbf{B}_R\mathbf{m}^{-1}\mathbf{B}_R^T$. Consequently, $\Gamma_{RS}=\mathbf{G}_{SR}\mathbf{G}_R^{-2}\mathbf{G}_{SR}^T$. This Γ_{RS} formula can be applied to properly compute projection matrices for STQN paths, which are steepest descent paths with \mathbf{R} determined from linearly independent combinations of redundant internal coordinates.

Case 3. For a distinguished reaction path (DRP) generated by energy minimizations with constrained values of coordinate τ , contained in \mathbf{S} ,

$$\Gamma_{RS}=\begin{bmatrix} \mathbf{X} & \mathbf{v} \\ \mathbf{v}^T & 1 \end{bmatrix}, \quad (14)$$

where \mathbf{X} is arbitrary,

$$\mathbf{v}=-\mathbf{F}_\tau^{-1}\mathbf{f}_\tau, \quad (15)$$

\mathbf{F}_τ is the quadratic force constant matrix in the \mathbf{S} representation with the τ row and τ column deleted, and \mathbf{f}_τ is the associated vector of force constants coupling τ to the remain-

ing coordinates. There is flexibility in the choice of \mathbf{X} because the gradient vector \mathbf{g}_S along a DRP has a nonzero element only in the τ position. A possible choice is

$$\mathbf{X}=(1-\alpha^2)\mathbf{I}-2\alpha^{-1}\sqrt{\mathbf{f}_\tau\cdot\mathbf{f}_\tau}\mathbf{F}_\tau^{-1}+\alpha^{-2}(\mathbf{f}_\tau\cdot\mathbf{f}_\tau)\mathbf{F}_\tau^{-2}+\alpha^2(\mathbf{f}_\tau\cdot\mathbf{f}_\tau)^{-1}\mathbf{f}_\tau\mathbf{f}_\tau^T, \quad (16)$$

for $0<\alpha<1$, and the corresponding Jacobian would be

$$\mathbf{J}=\begin{bmatrix} \sqrt{1-\alpha^2}\mathbf{I}+\alpha^{-1}\sqrt{\mathbf{f}_\tau\cdot\mathbf{f}_\tau}\mathbf{F}_\tau^{-1} & \alpha\mathbf{f}_\tau/\sqrt{\mathbf{f}_\tau\cdot\mathbf{f}_\tau} \\ \alpha\mathbf{f}_\tau^T/\sqrt{\mathbf{f}_\tau\cdot\mathbf{f}_\tau} & \sqrt{1-\alpha^2} \end{bmatrix}. \quad (17)$$

For a DRP, algebraic reduction of the projected force constant matrix \mathbf{F}_p of Eq. (13) simply gives the unprojected \mathbf{F} matrix with the (τ, τ) element replaced according to

$$F_{\tau\tau}\rightarrow\mathbf{v}^T\mathbf{F}_\tau\mathbf{v}=\mathbf{f}_\tau^T\mathbf{F}_\tau^{-1}\mathbf{f}_\tau. \quad (18)$$

In addition to its elegance, this DRP projection scheme is appealing because the complementary vibrational frequencies along the LAM path are invariant to the chemically meaningful choices of the internal coordinates for the modes orthogonal to the LAM coordinate. It is straightforward to prove that the mathematical condition for this invariance is that the transformation of complementary coordinates $\{T_i\}\rightarrow\{U_k\}$ is independent of τ , i.e., $(\partial U_k/\partial\tau)_T=0$. For internal rotation, this condition means that the complementary coordinates are localized in either the top or the frame and do not bridge the axis of rotation. Chemically meaningful complementary coordinates should generally satisfy this condition.

C. Cartesian projection scheme for IRP vibrational analysis

In the original reaction-path Hamiltonian formulation of Miller *et al.*,¹⁰ which was based partially⁵⁷ on the work of Hougen *et al.*,³ a rectilinear Cartesian projection scheme was employed to compute vibrational frequencies along IRPs. Let the mass-weighted Cartesian coordinates of the atoms in the molecule-fixed system be

$$\mathbf{q}_i=\sqrt{m_i}\mathbf{a}_i(s)+\boldsymbol{\xi}_i, \quad (19)$$

where $\{\mathbf{a}_i(s)\}$ and $\{\boldsymbol{\xi}_i\}$ correspond to motion along and away from the intrinsic reaction path, respectively. In addition to the center of mass and the Eckart equations,¹⁰ guaranteeing that no translation and no vibrational angular momentum arises during motion away from the path, the relation

$$\sum_{i=1}^N\sqrt{m_i}\mathbf{a}_i'(s)\boldsymbol{\xi}_i=0, \quad (20)$$

ensures that the normal vibrations are orthogonal to the intrinsic reaction coordinate. The composite $3N$ -dimensional tangent vector $[\sqrt{m_1}\mathbf{a}_1'(s), \sqrt{m_2}\mathbf{a}_2'(s), \dots, \sqrt{m_N}\mathbf{a}_N'(s)]$ is equal to $\mathbf{n}=-\nabla_q V/|\nabla_q V|$, the normalized gradient vector in mass-weighted Cartesian coordinates along the IRP. In the Cartesian projection scheme, the vibrational frequencies along the IRP are obtained by diagonalizing

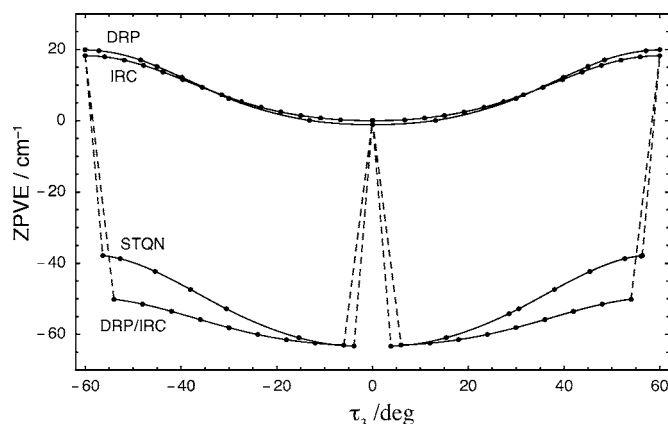


FIG. 3. Zero-point vibrational energy correction curves of acetaldehyde along different internal rotation paths, obtained at the RHF/6-31G(*d,p*) level. DRP= τ_3 constrained optimization path with case 3 internal projection scheme; IRC=intrinsic reaction path with IRC Cartesian projection scheme (numerically indistinguishable from case 1 internal projection); STQN=converged STQN path with IRC Cartesian projection scheme, as given by GAUSSIAN98 with keyword Freq(Projected); DRP/IRC= τ_3 constrained optimization path with IRC Cartesian projection scheme. All curves are referenced to the harmonic zero-point vibrational energy ($12\,992.9\text{ cm}^{-1}$) of the $\tau_3=0^\circ$ minimum, excluding the harmonic frequency of the $\nu_{15}(a'')$ methyl internal rotation mode.

$$\mathbf{K}_p = (\mathbf{I} - \mathbf{nn}^T)(\mathbf{I} - \mathbf{P}_{\text{trans,rot}})\mathbf{K}(\mathbf{I} - \mathbf{P}_{\text{trans,rot}})(\mathbf{I} - \mathbf{nn}^T), \quad (21)$$

where \mathbf{K} is the Hessian matrix in the \mathbf{q} space, and $\mathbf{P}_{\text{trans,rot}}$ is the well-known projection matrix for the three translations and three external rotations.^{10,53}

D. Comparison of $V_{\text{ZPVE}}(\chi)$ curves

The $V_{\text{ZPVE}}(\chi)$ curves obtained in this study for selected LAM paths are plotted in Fig. 3 in terms of the reference coordinate τ_3 . First, note that the IRC and τ_3 DRP curves are virtually identical, *provided* that the correct vibrational projection scheme for each path is employed. In the IRC case, either internal projection case 1 or Cartesian projection [Eq. (21)] may be invoked, the ZPVE results being numerically indistinguishable on the scale of the plot. Second, if the IRC Cartesian projection is applied along the τ_3 DRP, then the resulting ZPVE curve is $50\text{--}60\text{ cm}^{-1}$ below the proper result for the τ_3 path. Moreover, *apparent* discontinuities in this DRP/IRC $V_{\text{ZPVE}}(\chi)$ curve arise near the $\tau_3=0^\circ$ minimum and the $\tau_3=60^\circ$ transition state if comparisons are made to the usual $3N-6$ dimensional normal mode analyses at the stationary points. In reality, the DRP/IRC curve varies continuously around the stationary points, but the limiting ZPVE values are not equivalent to those from the proper IRC computation. Third, application of IRC Cartesian projection to the STQN path yields spurious results and characteristics similar to the DRP/IRC case, except that the apparent jump in $V_{\text{ZPVE}}(\chi)$ near the transition state is only about 40 cm^{-1} . A proper vibrational frequency analysis along the STQN path could employ internal projection case 2 above, with the rather complicated, automatically generated redundant internal coordinates of GAUSSIAN 98 for \mathbf{R} and a more conventional set \mathbf{S} as the computational basis.

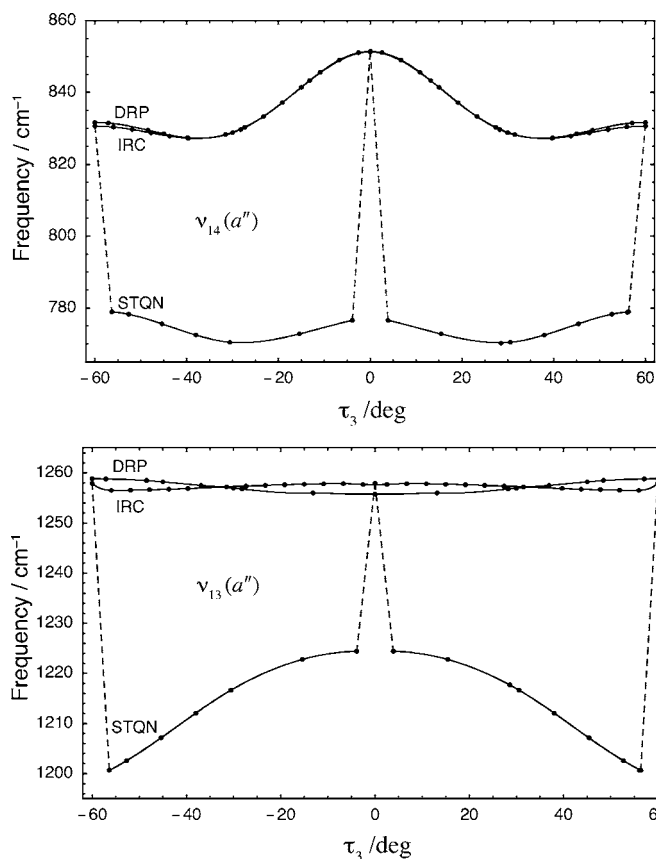


FIG. 4. Projected $\nu_{13}(a'')$ and $\nu_{14}(a'')$ harmonic frequencies of acetaldehyde along the different internal rotation paths. See caption of Fig. 3 for explanation of labels DRP, IRC, and STQN.

E. Comments on previous projected frequency results

In 2002 Xu *et al.*³² considered numerous issues, relevant to high-resolution spectroscopy, regarding the choice of LAM coordinates and the computation of projected vibrational frequencies along internal rotation paths. Toward the end of their analysis, they encountered an unexpected problem in computing projected vibrational frequencies with GAUSSIAN 98 for methyl rotations in acetaldehyde and methanol. In particular, they reported sizable discontinuities ($\sim 50\text{ cm}^{-1}$) in the vibrational frequencies for two out-of-plane bending modes of acetaldehyde as the internal rotation paths approached the stationary points. Albu and Truhlar³³ later examined the frequency discontinuities reported by Xu *et al.*³² By using the GAUSSRATE and POLYRATE computer programs,⁵⁸ they showed that no discontinuities should exist if IRC internal rotation paths are followed and either internal or Cartesian vibrational projection schemes appropriate for such paths are executed. They concluded that the jumps in vibrational frequencies reported in Ref. 32 “are not indicative of a theoretical deficiency in the formulation of the problem but rather of an unknown deficiency in the implementation used in the previous calculations.”

We succeeded in reproducing the problematic results of Xu *et al.*³² using both GAUSSIAN 98 and GAUSSIAN 03, as depicted in the ν_{13} and ν_{14} curves labeled STQN in Fig. 4. The same behavior observed in Fig. 3 for the STQN and

DRP/IRC $V_{\text{ZPVE}}(\chi)$ curves is exhibited for the individual ν_{13} and ν_{14} STQN frequencies. It is clear that the apparent discontinuities in the acetaldehyde frequencies are a consequence of using the GAUSSIAN 98 keyword Freq(Projected), appropriate for an IRC path, on geometries obtained along an STQN path. By using the programs GAUSSRATE and POLYRATE to map out the IRP, Albu and Truhlar³³ avoided mismatching the path with the projection scheme, and thus observed no apparent jumps in the vibrational frequencies. Our independent data, shown in Fig. 4, on the intrinsic reaction path with proper projection, also display smooth variations of vibrational frequencies along the internal rotation path. Of even greater interest here is the remarkable agreement in Fig. 4 between the IRC results and the τ_3 DRP curves generated with our simple internal projection scheme (case 3). For the acetaldehyde internal rotation prototype, the straightforward DRP method provides an almost perfect reproduction of the numerically more demanding IRC approach.

V. CONCLUSIONS

Each choice of LAM coordinate for internal rotation effectively constitutes a different adiabatic approximation for the separation of large- and small-amplitude motions. This work has clarified a number of issues concerning LAM coordinates and projected vibrational frequency computations along internal rotation paths, using the methyl rotation in acetaldehyde (CH_3CHO) as a model.

Among the four types of internal rotation paths considered here (ρ_1 DRP, τ_3 DRP, IRC, and STQN), only the τ_3 and IRC paths are recommended. Both the IRC path and the τ_3 DRP maintain threefold rotational symmetry for acetaldehyde internal rotation. The ρ_1 DRP has a clear symmetry deficiency, and the STQN path in redundant internal coordinates requires particular care in the construction of correct projection operators for vibrational analyses. Remarkably, the τ_3 and IRC paths are essentially indistinguishable for acetaldehyde, at least at the levels of electronic structure theory employed. Such congruence, if generally exhibited, may be of particular interest for large molecular systems, or high-accuracy computations. Although we have given a formulation of the τ_3 DRP path as a first-order differential equation, it is practically acquired by constrained optimization, which is a numerically stable and reliable method allowing points on a path to be determined independent of one another. Tracing an intrinsic reaction path is substantially more demanding, and integration over the IRC equation may not be stable, especially for internal rotation problems, that typically involve small forces. Additional advantages of the τ_3 DRP are lack of mass dependency, and desirable complementary coordinate invariance properties for both the path generation and vibrational frequency computations.

A unified internal coordinate projection scheme has been presented for determining complementary-mode vibrational frequencies, based on a generalized differential equation that governs both conventional LAM paths of steepest descent and those generated by constrained optimizations. This formulation exposes the dual coordinate dependence of the

zero-point vibrational energy correction to the internal rotation curve and the individual frequencies along the path. We stress that it is essential to match the vibrational projection scheme with the type of path to ensure valid results. For a DRP, algebraic reduction of our projected force constant matrix \mathbf{F}_P [of Eq. (13)] yields a remarkably simple prescription in which only the (τ, τ) element of the force constant matrix is changed. In the case of methyl rotation in acetaldehyde, this projection method for the τ_3 DRP gives a ZPVE modulation curve and small-amplitude vibrational frequencies in almost perfect agreement with the established internal and Cartesian projection procedures for the intrinsic reaction path. Of course, in more complicated systems in which the character of the internal rotation may substantially change over the range of large-amplitude motion, the IRP and DRP approaches may give noticeably different results. However, the congruence of the IRP and τ_3 DRP methods for the acetaldehyde prototype is indeed encouraging.

ACKNOWLEDGMENTS

Collaboration between Budapest, Hungary and Athens, Georgia was supported by U. S. National Science Foundation Grant No. INT-0312355, and by NATO Linkage Grant No. PST.CLG.979560. This research was also supported by the Hungarian Scientific Research Fund (Grant Nos. T047185 and T045955).

- ¹H. H. Nielsen, Phys. Rev. **40**, 445 (1932).
- ²J. D. Kemp and K. S. Pitzer, J. Chem. Phys. **4**, 749 (1936).
- ³J. T. Hougen, P. R. Bunker, and J. W. C. Johns, J. Mol. Spectrosc. **34**, 136 (1970).
- ⁴D. C. Moule and C. V. S. Ramachandra Rao, J. Mol. Spectrosc. **45**, 120 (1973).
- ⁵D. Papoušek, J. M. R. Stone, and V. Špirko, J. Mol. Spectrosc. **48**, 17 (1973).
- ⁶G. A. Natanson, Mol. Phys. **46**, 481 (1982).
- ⁷G. O. Sørensen, Top. Curr. Chem. **82**, 99 (1979).
- ⁸V. Szalay, J. Mol. Spectrosc. **128**, 24 (1988).
- ⁹K. A. Nguyen, C. F. Jackels, and D. G. Truhlar, J. Chem. Phys. **104**, 6491 (1996).
- ¹⁰W. H. Miller, N. C. Handy, and J. E. Adams, J. Chem. Phys. **72**, 99 (1980).
- ¹¹G. A. Natanson, B. C. Garrett, T. N. Truong, T. Joseph, and D. G. Truhlar, J. Chem. Phys. **94**, 7875 (1991).
- ¹²C. F. Jackels, Z. Gu, and D. G. Truhlar, J. Chem. Phys. **102**, 3188 (1995).
- ¹³A. R. Hoy and P. R. Bunker, J. Mol. Spectrosc. **52**, 439 (1974); **74**, 1 (1979).
- ¹⁴V. Špirko, J. Mol. Spectrosc. **101**, 30 (1983).
- ¹⁵V. Szalay, J. Mol. Spectrosc. **128**, 24 (1988).
- ¹⁶P. R. Bunker and P. Jensen, in *Computational Molecular Spectroscopy* (Wiley, Chichester, 2000), pp. 3–11.
- ¹⁷V. Szalay, A. G. Császár, and M. L. Senent, J. Chem. Phys. **117**, 6489 (2002).
- ¹⁸A. G. Ozkabak and L. Goodman, J. Chem. Phys. **96**, 5958 (1992).
- ¹⁹K. Fukui, Acc. Chem. Res. **14**, 363 (1981).
- ²⁰J. Villa and D. G. Truhlar, Theor. Chem. Acc. **97**, 317 (1997).
- ²¹D. Heidrich, in *The Reaction Path in Chemistry*, edited by D. Heidrich (Kluwer, Dordrecht, 1995), pp. 1–10.
- ²²P. R. Bunker and P. Jensen, *Molecular Symmetry and Spectroscopy*, 2nd ed. (NRC-CNRC, Ottawa, 1998).
- ²³A. G. Császár, V. Szalay, and M. L. Senent, J. Chem. Phys. **120**, 1203 (2004).
- ²⁴K. Fukui, J. Phys. Chem. **74**, 4161 (1970).
- ²⁵C. Gonzalez and H. B. Schlegel, J. Chem. Phys. **90**, 2154 (1989).
- ²⁶C. Gonzalez and H. B. Schlegel, J. Phys. Chem. **94**, 5523 (1990).
- ²⁷M. A. Collins, Adv. Chem. Phys. **93**, 389 (1996).
- ²⁸G. A. Natanson, Mol. Phys. **46**, 481 (1982).

- ²⁹D.-H. Lu and D. G. Truhlar, *J. Chem. Phys.* **99**, 2723 (1993).
- ³⁰G. A. Natanson, *Theor. Chem. Acc.* **112**, 68 (2004).
- ³¹D.-H. Lu, M. Zhao, and D. G. Truhlar, *J. Comput. Chem.* **12**, 376 (1991).
- ³²L. H. Xu, J. T. Hougen, R. M. Lees, and M. A. Mekhtiev, *J. Mol. Spectrosc.* **214**, 175 (2002).
- ³³T. V. Albu and D. G. Truhlar, *J. Mol. Spectrosc.* **219**, 129 (2003).
- ³⁴C. C. J. Roothan, *Rev. Mod. Phys.* **23**, 69 (1951).
- ³⁵C. Møller and M. S. Plesset, *Phys. Rev.* **46**, 618 (1934).
- ³⁶W. J. Hehre, R. Ditchfield, and J. A. Pople, *J. Chem. Phys.* **56**, 2257 (1972).
- ³⁷M. J. Frisch, G. W. Trucks, and H. B. Schlegel *et al.*, GAUSSIAN 98, Revision C.03, Gaussian, Inc., Pittsburgh PA, 1998.
- ³⁸M. J. Frisch, G. W. Trucks, and H. B. Schlegel *et al.*, GAUSSIAN 03, Revision B.01, Gaussian, Inc., Wallingford, CT, 2004.
- ³⁹P. Y. Ayala and H. B. Schlegel, *J. Chem. Phys.* **107**, 375 (1997).
- ⁴⁰A. A. Granovsky, <http://classic.chem.msu.su/gran/gamess/index.html>
- ⁴¹M. W. Schmidt, K. K. Baldridge, J. A. Boatz *et al.*, *J. Comput. Chem.* **14**, 1347 (1993).
- ⁴²J. F. Stanton *et al.*, ACES II. The package also contains modified versions of the MOLECULE Gaussian integral program of J. Almlöf and P. R. Taylor, the ABACUS integral derivative program written by T. U. Helgaker, H. J. A. Jensen, P. Jorgensen, and P. R. Taylor, and the PROPS property evaluation integral code of P. R. Taylor.
- ⁴³MATHEMATICA, Version 4 (Wolfram Research, Inc., Champaign, IL, 1999).
- ⁴⁴INTDER2005 is a general program developed by Wesley D. Allen and co-workers which performs various vibrational analyses and higher-order nonlinear transformations among force field representations.
- ⁴⁵W. D. Allen and A. G. Császár, *J. Chem. Phys.* **98**, 2983 (1993).
- ⁴⁶W. D. Allen, A. G. Császár, V. Szalay, and I. M. Mills, *Mol. Phys.* **89**, 1213 (1996).
- ⁴⁷G. Fogarasi, X. F. Zhou, P. W. Taylor, and P. Pulay, *J. Am. Chem. Soc.* **114**, 8191 (1992).
- ⁴⁸Y. G. Smeyers and M. Villa, *Chem. Phys. Lett.* **235**, 587 (1995).
- ⁴⁹M. Villa, Q. G. Herrera-Perez, and Y. G. Smeyers, *Chem. Phys. Lett.* **306**, 78 (1999).
- ⁵⁰C. Munoz-Caro, A. Nino, and D. C. Moule, *J. Mol. Struct.* **350**, 83 (1995).
- ⁵¹A. M. Halpern and E. D. Glendening, *J. Chem. Phys.* **119**, 11186 (2003).
- ⁵²A. Tachibana and K. Fukui, *Theor. Chim. Acta* **51**, 189 (1979).
- ⁵³E. B. Wilson Jr., J. C. Decius, and P. C. Cross, *Molecular Vibrations* (McGraw-Hill, New York, 1955).
- ⁵⁴Z. Kisiel, E. Bialkowska-Jaworska, L. Pszczolkowski, and H. Mäder, *J. Mol. Spectrosc.* **227**, 109 (2004).
- ⁵⁵S. Bell, *J. Mol. Struct.* **320**, 125 (1994).
- ⁵⁶L. Goodman, T. Kundu, and J. Leszczynski, *J. Am. Chem. Soc.* **117**, 2082 (1995).
- ⁵⁷G. A. Natanson, *Chem. Phys. Lett.* **190**, 209 (1992).
- ⁵⁸GAUSSRATE provides an interface between GAUSSIAN 03 and the program POLYRATE by J. C. Corchado, Y.-Y. Chuang, P. L. Fast *et al.*